THE 110 GHz ECH INSTALLATION ON DIII–D: STATUS AND INITIAL EXPERIMENTAL RESULTS

by

J. LOHR, R.W. CALLIS, R.C. O'NEILL,
D. PONCE, T.C. LUCE, M.E. AUSTIN,[1]
M. MURAKAMI,[2] and D. ZHANG[3]

THE 110 GHz ECH INSTALLATION ON DIII–D: STATUS AND INITIAL EXPERIMENTAL RESULTS

by

J. LOHR, R.W. CALLIS, R.C. O'NEILL,
D. PONCE, T.C. LUCE, M.E. AUSTIN,[1]
M. MURAKAMI,[2] and D. ZHANG[3]

[1]University of Texas at Austin
[2]Oak Ridge National Laboratory
[3]IPP, Academia Sinica

THE 110 GHz ECH INSTALLATION ON DIII–D: STATUS AND INITIAL EXPERIMENTAL RESULTS

J. LOHR, RW. CALLIS, R.C. O'NEILL, D. PONCE, T.C. LUCE
General Atomics, P.O. Box 85608, San Diego,
California 92186-5608, U.S.A.

M.E. AUSTIN
The University of Texas at Austin, Austin,
Texas 78712, U.S.A.

M. MURAKAMI
Oak Ridge National Laboratory, Oak Ridge,
Tennessee 37831, U.S.A.

D. ZHANG
Institute of Plasma Physics, Academia Sinica, Hefei,
Anhui, P.R.C.

Two 110 GHz gyrotrons with nominal output power of 1 MW each have been installed on the DIII–D tokamak. The gyrotrons, produced by Gycom and Communications and Power Industries, are connected to the tokamak by windowless evacuated transmission lines using circular corrugated waveguide carrying the HE_{11} mode. Initial experiments with the Gycom gyrotron showed good central heating efficiency at the second harmonic resonance with record central electron temperatures for DIII–D in excess of 10 keV achieved. The beam spot in the DIII–D vacuum vessel was well focused, with a diameter of approximately 8 cm, and it could be steered poloidally by a remotely adjustable mirror. The injection was at 19 deg off-perpendicular for current drive and the beams could be modulated for studies of energy transport and power deposition. The system will be described and the initial physics results will be presented. A third gyrotron, also at 110 GHz, will be installed later this year. Progress with this CPI tube will be discussed and future plans for the ECH installation and physics experiments using it will be presented.

1   Introduction

Two gyrotrons are installed and operating on the DIII–D tokamak. One, a Gycom Centaur tube [1,2] has been in routine service for about a year. The second, a VGT-8011A model [3] from Communications and Power Industries (CPI), has been operating for about a month. Both tubes are nominally 1 MW gyrotrons and produce rf at 110 GHz for full power pulse lengths which are limited by their output windows to 2 sec for the Gycom tube and 0.8 sec for the CPI tube. A second CPI gyrotron was damaged in testing at CPI and will be delivered to

General Atomics (GA) for installation in late 1997. The maximum test parameters for the installed tubes are listed in Table 1. In the case of the Gycom tube, the maximum pulse length achieved at GA has been 0.5 sec, a purely administrative limit. The CPI tube has only operated briefly with an evacuated transmission line and therefore no attempt to increase the pulse length has yet been made.

Table 1: Gyrotron Parameters

	Gycom Centaur	CPI VGT-8011A
Frequency	110.10–109.75 GHz	110.03–109.95 GHz
Output power	0.926 MW	0.905 MW
Max. pulse length, full power	2.0 sec	0.8 sec
Max. pulse power	1.2 MW at 2.0 msec	1.013 MW at 2.0 msec
RF efficiency	38%	32%
Operating current	34 A	35 A
Gun anode voltage	N/A	30 kV
Internal mode	$TE_{19,5}$	$TE_{22,6}$
Output mode	$HE_{1,1}$	$HE_{1,1}$
Peak cavity Ohmic loss	$\leq 2.0\ kW/cm^2$	$\leq 2.0\ kW/cm^2$

2   Transmission Lines

The rf power is delivered from the gyrotrons to the DIII-D tokamak by evacuated windowless transmission lines about 40 m in length. The waveguide lines incorporate forward/reverse power flow monitoring in a miter bend and can generate any arbitrary elliptical polarization by reflection from ribbed mirrors in two of the miter bends. The lines include switches for routing the power to dummy loads capable of absorbing the full gyrotron output power for up to 2 sec, manual and pneumatically operated vacuum valves, vacuum pump connections, and a fast shutter system for protecting the tokamak in case of a vacuum failure in the line. The waveguide lines carry the $HE_{1,1}$ mode, which couples well to the free space Gaussian, permitting a simple launcher to be used in the tokamak. The transmission lines are presented to scale in Fig. 1.
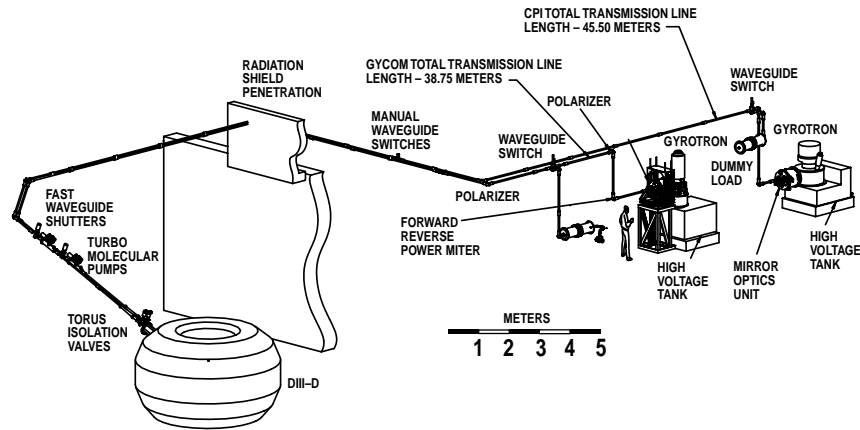
Figure 1. Scale drawing of the DIII–D gyrotron and transmission line layout. The waveguides are 31.75 mm diameter circular corrugated lines and carry the $HE_{1,1}$ mode. A third line is being installed for operation by the end of summer 1997.

In principle, the gyrotrons can operate continuously except for the weak links in the system, the gyrotron output windows. The window in the case of the Gycom gyrotron is an edge cooled disk of boron nitride, which can be operated at temperatures up to 900 K. The CPI gyrotrons both employ double disk sapphire windows cooled by FC-75, a low loss chloro-fluorocarbon fluid. FC-75 boils at about 120°C and this temperature in turn limits the pulse length to 0.8 sec. The designers of both tubes increased the power handling capability of their windows by flattening the Gaussian beam in the internal mirror system and spreading the power more uniformly over the window area. The non-Gaussian modes which are added to the beam in order to achieve this flattened Gaussian are reformed into the main gaussian beam by correction mirrors in the Matching Optics Unit (MOU) an evacuated chamber attached directly to the gyrotron output flange.

The MOUs are pumped by turbomolecular pumps to pressures in the low 10^{-6} torr range and incorporate ZnSe windows so that the gyrotron window temperatures can be monitored by infrared pyrometers. The MOUs also incorporate window arc detection, rf monitor pickoffs, and micrometers for precise alignment of the mirrors. In order to avoid placing mechanical strains on the gyrotrons, the entire MOU assemblies are floating on springs. The MOU mirrors focus the gyrotron output beams onto the input end of the 31.75 mm diameter corrugated waveguide. Transverse alignment to accuracy of about 0.1 mm and coaxiality to about 0.1 deg are required at the waveguide to ensure coupling to the guide with

minimal mode conversion [4,5]. In Fig. 2 the MOU and burn paper patterns are shown for the first short section of waveguide at the output of the MOU on the Gycom system.

The small diameter waveguide employed represents a compromise between power handling capability and immunity to misalignment and motion of the line. But the requirements for accurately steering the beam into the waveguide, particularly if phase correcting mirrors are installed to form the Gaussian, makes it desirable to mount the MOU so that the beam enters on the optical beam trajectory and therefore hits the first mirror at its center. Free space measurements of the beam trajectory angle and position at the output window were made and then special adapter flanges were manufactured to accomplish this aspect of the alignment. The Gycom beam exited the window with a 0.31 deg up tilt 4.4 mm above the window center and the CPI beam exited perpendicularly to within 0.05 deg but offset 6.4 mm below and 5.5 mm right of the window axis.

3 In-Vessel Testing

Inspection of the DIIID launcher assembly following operation of the Gycom gyrotron earlier this year revealed signs of arcing on the face of the poloidal steering mirror. This mirror was graphite coated by a 0.15 µm layer of tungsten and overcoated by a 2.0 µm layer of copper to avoid eddy current induced mechanical loading during disruptions. The copper and tungsten had been removed along dendritic tracks at the rf beam strike point. Relaxation of the DIII–D disruption requirements, primarily for the maximum current disruption anticipated, permitted the replacement of the graphite mirrors with solid copper mirrors 3.2 mm thick mounted on a stainless steel support structure. Following installation of the refurbished launcher assembly, new measurements of the beams in the vacuum vessel were made.

Both gyrotron and waveguide systems were tested at atmospheric pressure by propagating short pulses to the DIII–D vacuum vessel during a maintenance vent. A paper target was positioned vertically at the radial geometric center of the vessel with its plane perpendicular to the azimuthal component of the beam trajectory from the launcher. The target was viewed by infrared and visible cameras and the gyrotrons were pulsed for 150–500 µsec pulses at pulse repetition frequencies between 0.5 and 8.0 Hz. A videotape was made which permitted subsequent
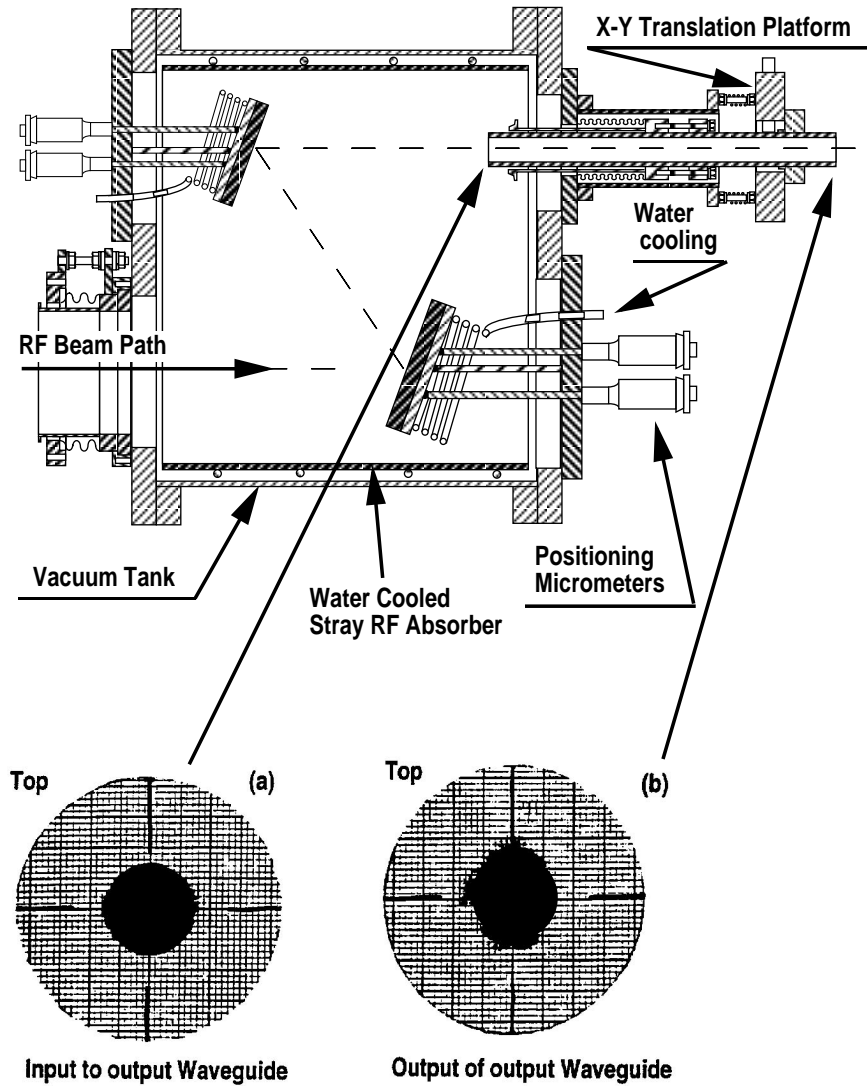
Figure 2. Matching optics unit and burn paper patterns for the Gycom installation. The first mirror provides phase correction to form a Gaussian beam and the second mirror focuses the beam onto the waveguide input. The mirrors are micrometer adjustable and the entire assembly is evacuated to pressures in the low 10^{-6} torr range.

analysis of the location and shape of the beam in the chamber for different angular positions of the flat poloidally scanning mirrors.

The scanning mirrors are both angled 19 deg off-perpendicular for current drive and rotate together to scan the beams poloidally. This geometry causes the two beams to encounter the EC resonance at different elevations with respect to the midplane, although it is possible to set the alignment so that the beams are at the same elevation for one poloidal scan angle. In the present case, it was decided to estimate the location of the $q = 1.5$ surface for usual plasmas and to make this be the elevation at which both beams cross the same horizontal plane at the EC resonance. This plane is about 60 cm above the midplane. In Fig. 3 the beams are shown in the infrared striking the paper target at this elevation. At the midplane the two beams are separated by 15 cm vertically, or about twice the full width at half maximum for a single beam as discussed below.

Pulsing the rf at duty cycles differing by a factor of approximately 2.7 permitted the target heating to be related to a Gaussian beam profile. The results of this analysis are shown in Fig. 4, where it is seen that the Gycom system generates an approximately Gaussian beam with full width at half maximum of about 8 cm, which is in agreement with the launcher optical design calculations. The CPI beam has a kidney shape and appears to diverge more rapidly with distance than the Gycom beam. Very little attention has been paid to the alignment of the CPI system and the offset adapter flange was not installed when Fig. 4 was made, therefore the beam shape in the figure should not imply anything about the ultimate beam quality. When a target was placed directly in front of the poloidal steering mirror, both beams were observed with the IR camera to be quite circular and virtually free of sidelobes.

From the operating regimes, the duty cycles used, and the infrared response it was estimated that both tubes were generating about 400 kW and that both transmission lines were working as expected. At atmospheric pressure and relatively high power the pulse lengths were limited by breakdown to about 500 µsec in length. Testing at full power and pulse length will only be possible when the line is evacuated.

4   Experimental Program

The Gycom gyrotron was used early in 1996 in preliminary physics experiments on DIII–D. In these experiments pulse lengths of 500 msec were used since the tube
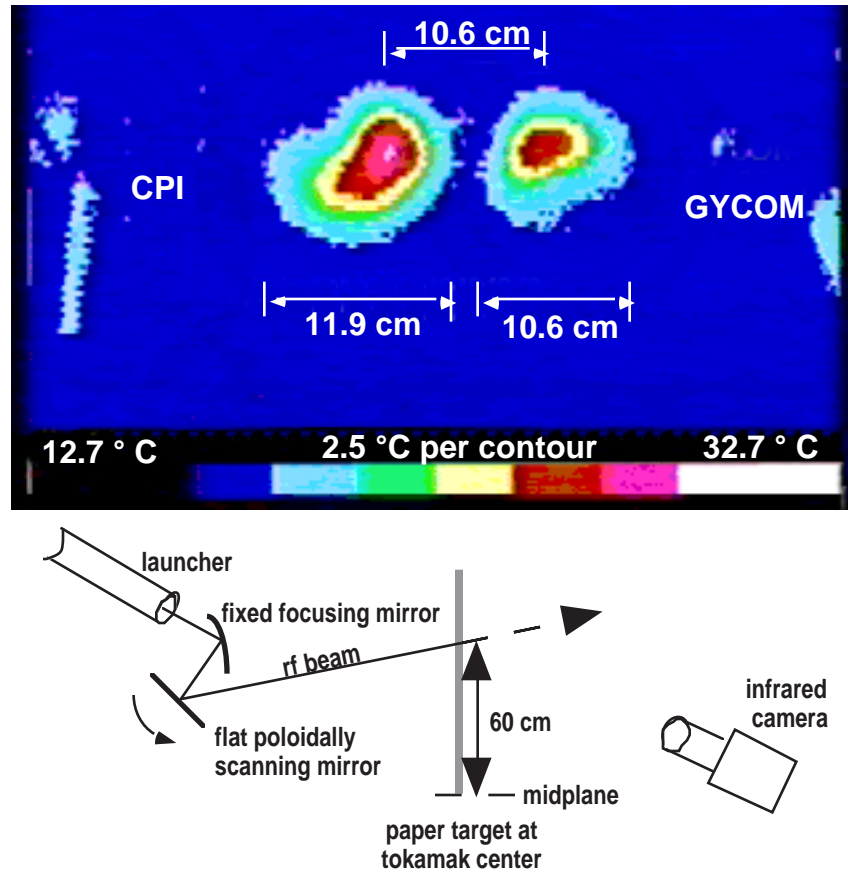
Figure 3. Infrared image of the Gycom and CPI rf beams passing through and heating a paper target in the DIII–D vacuum vessel. The target is at an elevation of 60 cm, corresponding to $q \sim 1.5$ in a standard DIII–D plasma.

had not been qualified for longer pulses. About 0.5 MW was injected into the DIII–D plasma. Both continuous and pulse modulated operation were tested.

In the first tests, at low target density and about 0.5 MW injected, DIII–D record electron temperatures of over 10 keV were achieved. An electron temperature profile generated from both Thomson scattering and ECE data using the Michelson interferometer is presented in Fig. 5 along with the time dependence of
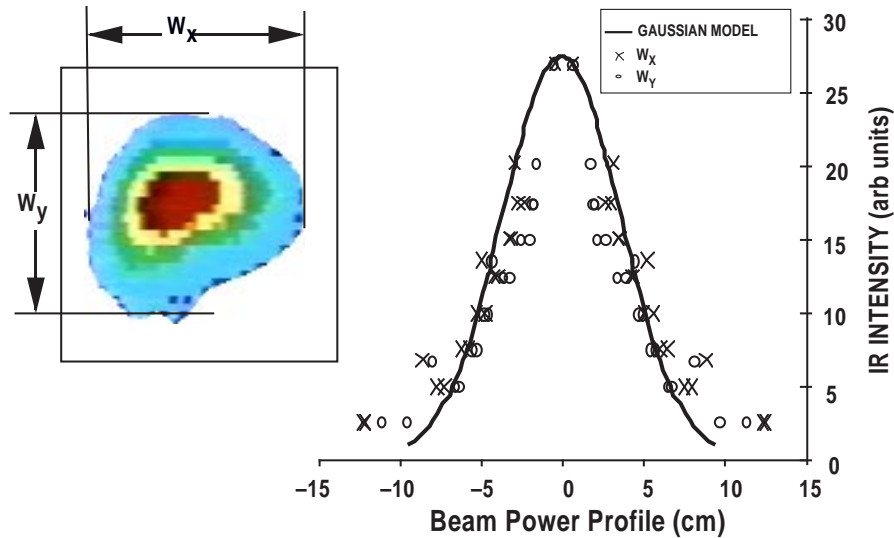
Figure 4. Infrared images of the beam were obtained for duty cycles differing by factors of e, 2.7. These data permit the profiles to be fitted by a Gaussian beam model and indicate that the Gaussian beam diameter is about 8 cm, consistent with the optics calculations for the launcher system. The beam waist is actually close to the launcher and weak focusing is used to give a slightly diverging beam.

several relevant plasma parameters. The experiment attempted to investigate the synergistic increase in fast wave current drive at high electron temperatures. Despite the extremely high target temperatures, themselves representing a successful result, the synergism with fast wave current drive was not observed, since it proved to be impossible to maintain the required low densities during the fast wave injection, as seen on the time traces. There is approximately a linear tradeoff between T_e and n_e in ECH experiments, so it is anticipated that combining the powers from two, and later this year, three gyrotrons will enable the high target temperature to be maintained in spite of this density increase and the fast wave current drive will increase proportionately.

Initial testing of the Gycom ECH system included measurements of the power deposition profile in the plasma. This was done in two ways, both of which made use of the 32-channel heterodyne ECE system. In the first analysis, the slopes of the ECE signals in the first few msec following turn-off of the rf power were used to infer the deposition profile. At each location in the plasma the temperature,
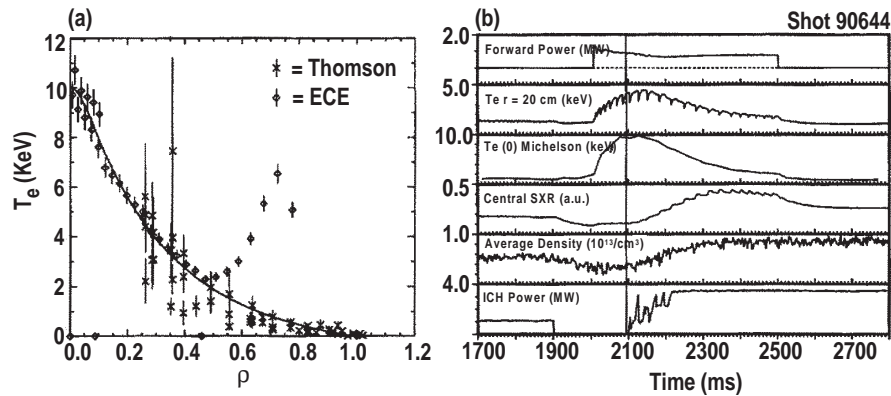
Figure 5. (a) T_e profile for low density target plasma with about 500 kW injected and central resonance. The ECE data indicate a superthermal tail was present at this low density. The central T_e value is a record for DIII–D.(b) Time dependence of relevant parameters for fast wave synergy experiment. The profile in (a) was obtained at the time indicated by the vertical lines.

hence the ECE signal, is determined by the balance between local power absorption and diffusive power flow. Because the power deposition can be stopped quickly compared with diffusion, the ECE response just after removal of the heating power is indicative of the power which was being deposited.

This analysis indicated that the power deposition profile was somewhat broader than expected from the profile of Fig. 4. In Fig. 6 the profile from this analysis is plotted. The full width at half maximum for the inferred power deposition profile is about 14 cm, compared with the value of about 8 cm measured with the IR camera analysis. The ECE data also have somewhat broader wings than expected from the IR data.

The second analysis was performed for modulated ECH power and used a Fourier transform analysis to obtain the amplitude and phase of the heat pulses propagating away from the point of deposition. The broader profile in Fig. 6 shows the result of the harmonic analysis. For this analysis the modulation frequency was 50 Hz, at a modulation depth of 60%, obtained by a 13% modulation of the gyrotron beam voltage.

The relatively low modulation frequency 50 Hz used in the Fourier analysis makes it difficult to separate transport effects from the effects of the power deposition profile. Sawteeth at or near the modulation frequency can also complicate
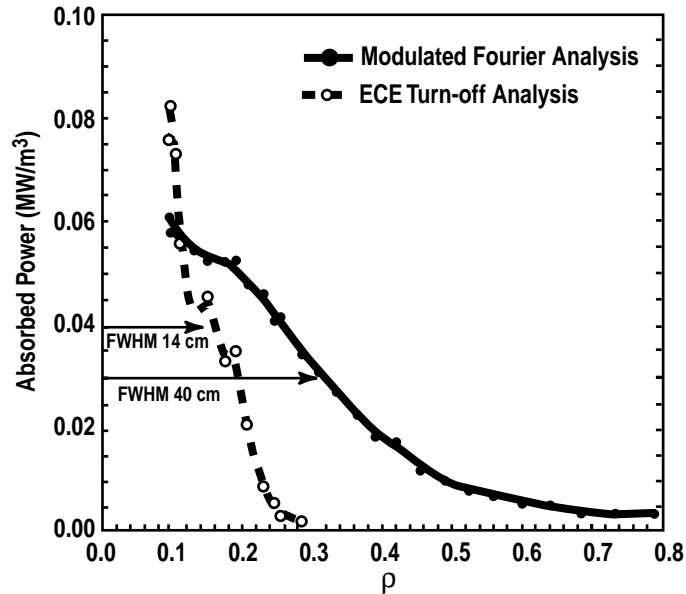
Figure 6 Power deposition profile from ECE signals, for modulated and unmodulated ECH. The power deposition profiles from these analyses are also broader than indicated by the IR camera measurements of heating of the paper target.

the analysis. For the next series of experiments, modulation at frequencies up to about 1 kHz will be used.

One explanation for the discrepancy between the power deposition profiles measured with the paper target and in plasma could be that the proper elliptical polarization for the 19 deg injection angle is not being obtained in the launched beam. The gyrotron output polarization was measured to be horizontal and linear as expected, but polarimeter measurements made using a pickoff hole in the last miter mirror before the tokamak were inconclusive. Injection of a fraction of the power in the O–mode, for which the single pass absorption is poor, could result in a broad deposition profile. Since the IR measurements did not indicate sidelobes in the launched beam or a broader than expected profile, a new polarimeter is being prepared to measure the polarization of the launched beam.

The 1997 DIII–D experimental schedule has been announced and nearly half of the planned experiments will make use of the ECH installation. Initial work will verify the basic physics of ECH and ECCD, for which efficiencies will be determined as a function of position, or normalized flux, in the plasma. As part of

this initial work, modulated ECH will be used to continue work on the heat pinch effect seen earlier in off-axis heating experiments. As discussed above, the ECH/fast wave synergy experiment, made possible by the increase in available ECH power above 1 MW, will also be done.

In the transport arena, a series of experiments is planned to investigate transport theories. These experiments will make use of the rapid heating of electrons only by ECH, since the theories have different predictions for plasma response to rapid transients. The fact that ECH injects neither particles nor momentum makes it ideal for tests of theories of transport barrier formation, which differ in their treatment of momentum and rotation. It is known from earlier work that an L-H transition can be induced by ECH with about the same threshold power requirements as for neutral beams, but the relative precision with which ECH power can be applied spatially may reveal changes in the threshold power for H–mode depending upon power deposition location.

Stability and control of MHD modes should be able to be addressed using ECH to stabilize neoclassical tearing modes and the effect of edge resonant ECH on ELMs, seen earlier in poorly controlled experiments can now be done under much improved experimental conditions. Finally, non-inductive startup, current transport during MHD activity and a variety of scaling experiments are planned.

5   Conclusion

The DIII–D ECH installation now consists of two operating gyrotrons with a third expected to be installed by the end of 1997. The transmission lines and ancillary equipment are working well with good efficiency and the launcher is performing as expected. An ambitious series of experiments is planned for the 1997 campaign.

References

1. M.V. Agapova, V.V. Alikaev, L.A. Axenova, *et.al.*, in *Proc. 20th Int. Conf. on Infrared and Millimeter Waves*, Cocoa Beach, Florida, ed. R. Temkin (1995), p. 205.

2. John Lohr, Dan Ponce, L. Popov, *et.al.*, in *Proc. 3rd Int. Workshop on Strong Microwaves in Plasmas*, Moscow/St. Petersburg, Russia (1996).

3. Kevin Felch, Monica Blank, Philipp Borchard, *et.al.*, in *IEEE Trans. Plasma Sci.* **24**, 558 (1996).

4. John L. Doane, *Infrared and Millimeter Waves* **13**,123 (1985).

5. K. Ohkubo, in *Proc. US/Japan RF Technology Exchange* (1995), unpublished.